

Development of Life Prediction Models for High Strength Steel in a Hydrogen Emitting Environment

**by Scott M. Grendahl, Franklyn Kellogg,
Hoang Nguyen, and Matthew Motyka**

ARL-TR-6006

May 2012

NOTICES

Disclaimers

The findings in this report are not to be construed as an official Department of the Army position unless so designated by other authorized documents.

Citation of manufacturer's or trade names does not constitute an official endorsement or approval of the use thereof.

Destroy this report when it is no longer needed. Do not return it to the originator.

Army Research Laboratory

Aberdeen Proving Ground, MD 21005-5069

ARL-TR-6006

May 2012

Development of Life Prediction Models for High Strength Steel in a Hydrogen Emitting Environment

Scott M. Grendahl

Weapons and Materials Research Directorate, ARL

Franklyn Kellogg, Hoang Nguyen, and Matthew Motyka
Data Matrix Solutions, Inc.

REPORT DOCUMENTATION PAGE				Form Approved OMB No. 0704-0188	
Public reporting burden for this collection of information is estimated to average 1 hour per response, including the time for reviewing instructions, searching existing data sources, gathering and maintaining the data needed, and completing and reviewing the collection information. Send comments regarding this burden estimate or any other aspect of this collection of information, including suggestions for reducing the burden, to Department of Defense, Washington Headquarters Services, Directorate for Information Operations and Reports (0704-0188), 1215 Jefferson Davis Highway, Suite 1204, Arlington, VA 22202-4302. Respondents should be aware that notwithstanding any other provision of law, no person shall be subject to any penalty for failing to comply with a collection of information if it does not display a currently valid OMB control number. PLEASE DO NOT RETURN YOUR FORM TO THE ABOVE ADDRESS.					
1. REPORT DATE (DD-MM-YYYY) May 2012		2. REPORT TYPE Final		3. DATES COVERED (From - To) 1 January 2010–31 December 2010	
4. TITLE AND SUBTITLE Development of Life Prediction Models for High Strength Steel in a Hydrogen Emitting Environment				5a. CONTRACT NUMBER	
				5b. GRANT NUMBER	
				5c. PROGRAM ELEMENT NUMBER	
6. AUTHOR(S) Scott M. Grendahl, Franklyn Kellogg, * Hoang Nguyen, * and Matthew Motyka *				5d. PROJECT NUMBER WP-2152	
				5e. TASK NUMBER	
				5f. WORK UNIT NUMBER	
7. PERFORMING ORGANIZATION NAME(S) AND ADDRESS(ES) U.S. Army Research Laboratory ATTN: RDRL-WMM-F Aberdeen Proving Ground, MD 21005-5069				8. PERFORMING ORGANIZATION REPORT NUMBER ARL-TR-6006	
9. SPONSORING/MONITORING AGENCY NAME(S) AND ADDRESS(ES)				10. SPONSOR/MONITOR'S ACRONYM(S) SERDP	
				11. SPONSOR/MONITOR'S REPORT NUMBER(S)	
12. DISTRIBUTION/AVAILABILITY STATEMENT Approved for public release; distribution is unlimited.					
13. SUPPLEMENTARY NOTES *Data Matrix Solutions, Inc.					
14. ABSTRACT Solvent substitution for maintenance and overhaul operations of military systems has been a primary environmental concern for many years. Cadmium replacement in these systems has been targeted for decades. Both of these areas have a common obstacle for implementation of any potential alternative. Hydrogen embrittlement of high strength steel is the most predominant unforeseen hurdle since high strength materials show sensitivity to the phenomena and the source of the hydrogen can be anything within the fabrication process, maintenance practice, or the natural corrosion cycle. Standardized testing on this issue has traditionally stemmed from the aerospace industry where it is a principal focus. Historically, the various aerospace defense contractors have each tested in their own manner, which has led to the national standard incorporating many approved test geometries and “grey” procedures. This work evaluated hydrogen susceptibility over a range of material strength, load level, and hydrogen emitting environment (weight-percent sodium chloride [NaCl]) which demonstrated performance with parameter ranges, not as “pass/fail” results, while developing life predictive models for each geometry.					
15. SUBJECT TERMS hydrogen embrittlement, 4340, corrosion					
16. SECURITY CLASSIFICATION OF:			17. LIMITATION OF ABSTRACT	18. NUMBER OF PAGES	19a. NAME OF RESPONSIBLE PERSON
a. REPORT	b. ABSTRACT	c. THIS PAGE			Scott M. Grendahl
Unclassified	Unclassified	Unclassified	UU	48	19b. TELEPHONE NUMBER (Include area code) 410-306-0819

Contents

List of Figures	iv
List of Tables	v
Acknowledgments	vi
1. Introduction	1
2. Objective	1
3. Materials	2
3.1 Heat Treating.....	3
3.2 Cadmium Plating.....	4
4. Experimental Procedures	6
4.1 DoE.....	6
4.2 Specimens, Environments, and Loading Procedure.....	8
5. Results	12
6. Discussion	26
7. Conclusions	27
Appendix A. 1a.1 Raw Data	29
Appendix B. 1a.2 Raw Data	31
Appendix C. 1c Raw Data	33
Appendix D. 1d Raw Data	35
Appendix E. 1e Raw Data	37
Distribution List	39

List of Figures

Figure 1. ASTM-F-519 specimen geometries.	2
Figure 2. Masking/plating of the five specimen geometries.	5
Figure 3. Cadmium plated experimental specimens (top to bottom; 1a.1, 1a.2, 1c, 1d, and 1e).	9
Figure 4. Geometry 1a.1 and 1a.2 in-situ environmental setup. A) the empty container, B) the sample in the cup, C) the sample loaded onto the mechanical test frame, and D) the sample being tested in solution.	10
Figure 5. Geometry 1c in-situ environmental setup. A) loaded, B) loaded and masked, and C) being tested in solution.	10
Figure 6. Geometry 1d in-situ environmental setup. A) loaded, B) loaded and masked, C) being tested in solution, and D) top-down perspective.	11
Figure 7. Geometry 1e in-situ environmental setup. A) loaded, B) loaded and masked, and C) being tested in salt water.	11
Figure 8. Final 1a.1 specimen geometry life prediction models.	21
Figure 9. Final 1a.2 specimen geometry life prediction models.	22
Figure 10. Final 1c specimen geometry life prediction models.	23
Figure 11. Final 1d specimen geometry life prediction models.	24
Figure 12. Final 1e specimen geometry life prediction models.	25

List of Tables

Table 1. Temper lot quantities.	4
Table 2. Design of experiment conditions matrix.....	6
Table 3. Linear portion test matrix.	7
Table 4. Quadratic portion test matrix.	7
Table 5. Confirmation portion test matrix.	8
Table 6. Preliminary 1a.1 equation parameter analysis estimates.	14
Table 7. Final 1a.1 equation parameter analysis estimates.	14
Table 8. Preliminary 1a.2 equation parameter analysis estimates.	15
Table 9. Final 1a.2 equation parameter analysis estimates.	16
Table 10. Preliminary 1c equation parameter analysis estimates.	17
Table 11. Final 1c equation parameter analysis estimates.	17
Table 12. Preliminary 1d equation parameter analysis estimates.	18
Table 13. Final 1d equation parameter analysis estimates.....	19
Table 14. Preliminary 1e equation parameter analysis estimates.	20
Table 15. Final 1e equation parameter analysis estimates.	20

Acknowledgments

The authors wish to thank Mr. Ed Babcock, Mr. Steven Gaydos, Mr. Joseph Osborne, Mr. Stephen Jones and Ms. Shuying Zhu of The Boeing Company for fruitful discussions and analysis of the data presented within this work. Mr. Richard Green of Green Specialty Service and Mr. Craig Willan of Omega Research Inc. are acknowledged for the material specimens and their support of this work.

1. Introduction

Solvent substitution for maintenance and overhaul operations of military systems has been a primary environmental concern for many years. Cadmium replacement in these systems has been targeted for decades. Both of these areas have a common obstacle for implementation of any potential alternative. Hydrogen embrittlement of high strength steel is the most predominant unforeseen hurdle since high strength materials show sensitivity to the phenomena and the source of the hydrogen can be anything within the fabrication process, maintenance practice, or the natural corrosion cycle. Standardized testing on this issue has traditionally stemmed from the aerospace industry where it is a principal focus. Historically, the various aerospace defense contractors have each tested in their own manner, which has led to the national standard incorporating many approved test geometries and “grey” procedures. This standardized test is a “pass/fail,” “go/no-go” type test and the “grey” procedures lead directly to conflicting test results and perceived risk and/or roadblocks when it comes to implementing proposed alternative chemicals and coatings. This work evaluated hydrogen susceptibility over a range of material strength, load level, and hydrogen emitting environment (weight-percent sodium chloride [NaCl]) which demonstrated performance with parameter ranges, not as “pass/fail” results, while developing life predictive models for each geometry. This should greatly increase the applications for which the replacements will be considered, as the models provide the acceptability criteria for the parameters specific to each application.

2. Objective

This work was designed to utilize a “Design of Experiment” (DoE) approach to create life prediction models for air-melted SAE-AMS-6415 steel using common ASTM-F-519 specimen geometries in combination with load cell measurement and time monitored experiments.^{1,2} The geometry that proved the most viable and reliable was determined from the data. It will be subsequently used to evaluate the most prospective environmentally friendly maintenance chemicals and cadmium alternative coatings that currently have their use limited via the perceived risk of hydrogen embrittlement.³

¹SAE-AMS-6415S-2007. *SAE World Headquarters* **2007**.

²ASTM F 519-10. *ASTM International* **2010**.

³MIL-STD-870C. *Department of Defense* **2009**.

3. Materials

The five specimen geometries used, fabricated from SAE-AMS-6515 air-melted steel, were manufactured in accordance with the geometries of ASTM-F-519 1a.1, 1a.2, 1c, 1d, and 1e specimens. These specimens are commonly used by nearly all of the aerospace industry and technical community for conducting hydrogen embrittlement research. They are depicted in figure 1.

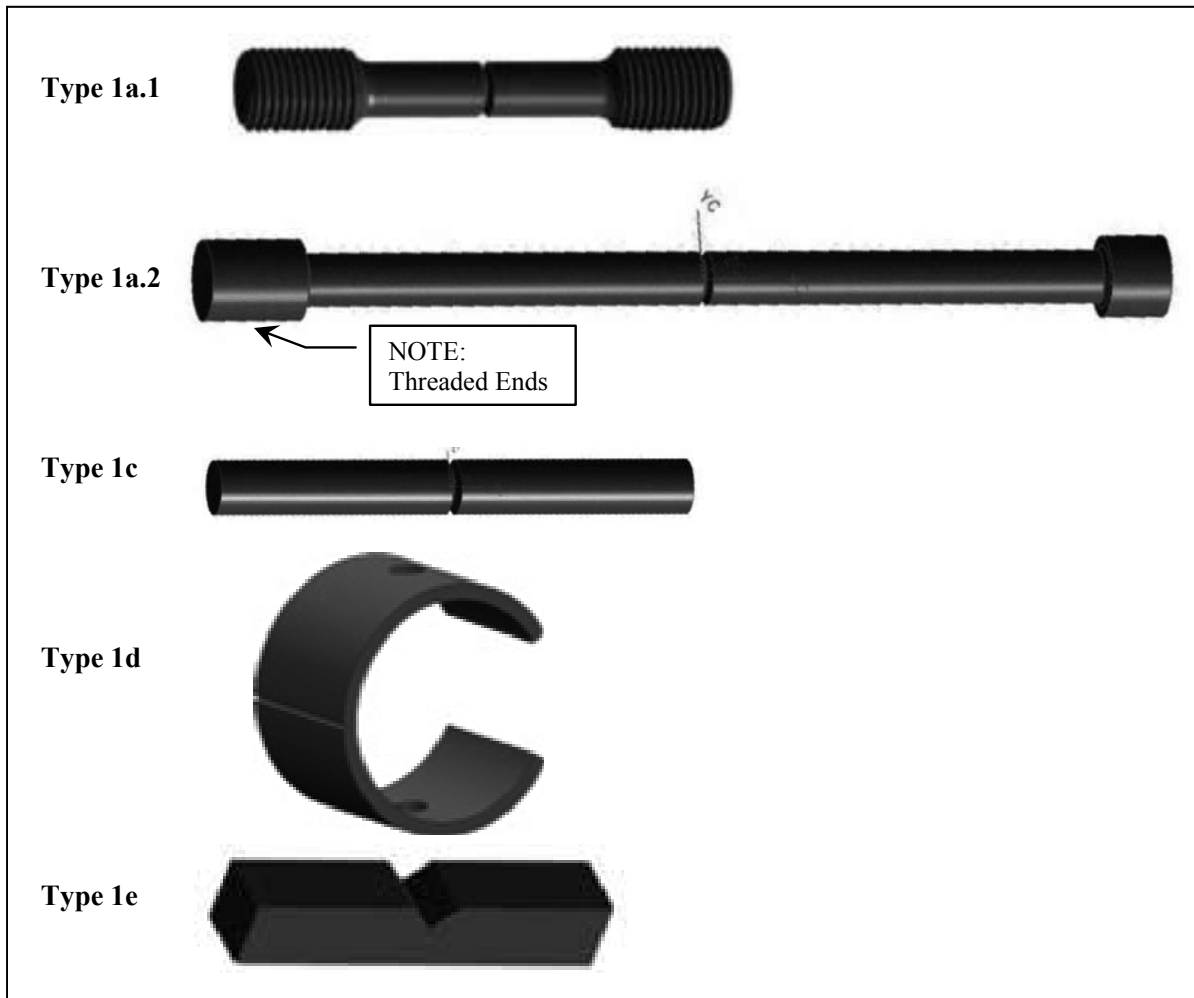


Figure 1. ASTM-F-519 specimen geometries.

3.1 Heat Treating

A critical element in conducting this comparative research across the five geometries was to have the material strength as close to identical as possible. This proved tedious as the stock removal differs on each specimen geometry in blanking and final machining. Additionally, production heat treating proved an imprecise process without tight control. Suppliers were not used to keeping such tight tolerances on their heat-treated product. It was crucial to have the strength level of each specimen in a very narrow range (± 5 ksi), otherwise data variation based on geometry might not be observable in the output. The team constructed a sub-matrix for the background work. This process entailed certification of a rack-basket, hardening furnace, and tempering furnace by normalizing, hardening, and tempering samples to 280 ksi utilizing small cylindrical buttons for in-process hardness tests and verification tensile samples. Once tested, verified and certified per mutually-agreed parameters, furnaces and ovens had the process frozen for approval. The heat treatments of the actual specimens were completed within 30 days of the date of frozen planning approval. There were five heat treatment batches for this work across five ASTM-F-519 specimen geometries 1a.1, 1a.2, 1c, 1d, and 1e. Each batch of specimens, T1 through T5, required heat treatment in accordance with the following:

- T1 = 140 ± 5 ksi (135–145 ksi)
- T2 = 158 ± 5 ksi (153–163 ksi)
- T3 = 210 ± 5 ksi (205–215 ksi)
- T4 = 262 ± 5 ksi (257–267 ksi)
- T5 = 280 ± 5 ksi (275–285 ksi)

The specimen counts varied by temper level following the overall design of experiments. The specimens were heat treated in batches according to their temper lot designation depicted in table 1. The individual quantities were derived from the DoE matrix further explained in the experimental procedures section.

- T1 = 30 + 6 tensiles
- T2 = 75 + 6 tensiles
- T3 = 180 + 6 tensiles
- T4 = 75 + 6 tensiles
- T5 = 45 + 6 tensiles

Table 1. Temper lot quantities.

Temper Lot No.	Strength Target (ksi)	No. of Specimens							
		1a.1	1a.2	1c	1d	1e	Total	+	Tensiles
T1	140	6	6	6	6	6	30	+	6
T2	158	15	15	15	15	15	75	+	6
T3	210	36	36	36	36	36	180	+	6
T4	262	15	15	15	15	15	75	+	6
T5	280	9	9	9	9	9	45	+	6

3.2 Cadmium Plating

The plating requirements were critical since the surface area plated affects both the amount of hydrogen introduced into the sample and the free path out of the sample during hydrogen embrittlement (HE) bake relief. Specimens were supplied in the stress relieved condition to an aerospace industry approved cadmium plating vendor. The cadmium plating was low hydrogen embrittling (LHE) cadmium in accordance with MIL-STD-870 Rev. C. Type II, Class 1.⁴ The threads were masked and the specimens were post processed baked at 375 ± 25 °F within 1 h of plating. Plating requirements were set so that each specimen would have an equivalent surface area to volume ratio during environmental testing, but were largely dependent on the allowable container size for holding the test fluid. The plating requirements were set so that no fluid would contact bare un-plated steel during testing. The plated area of the specimens was in accordance with figure 2.

⁴ Ibid.

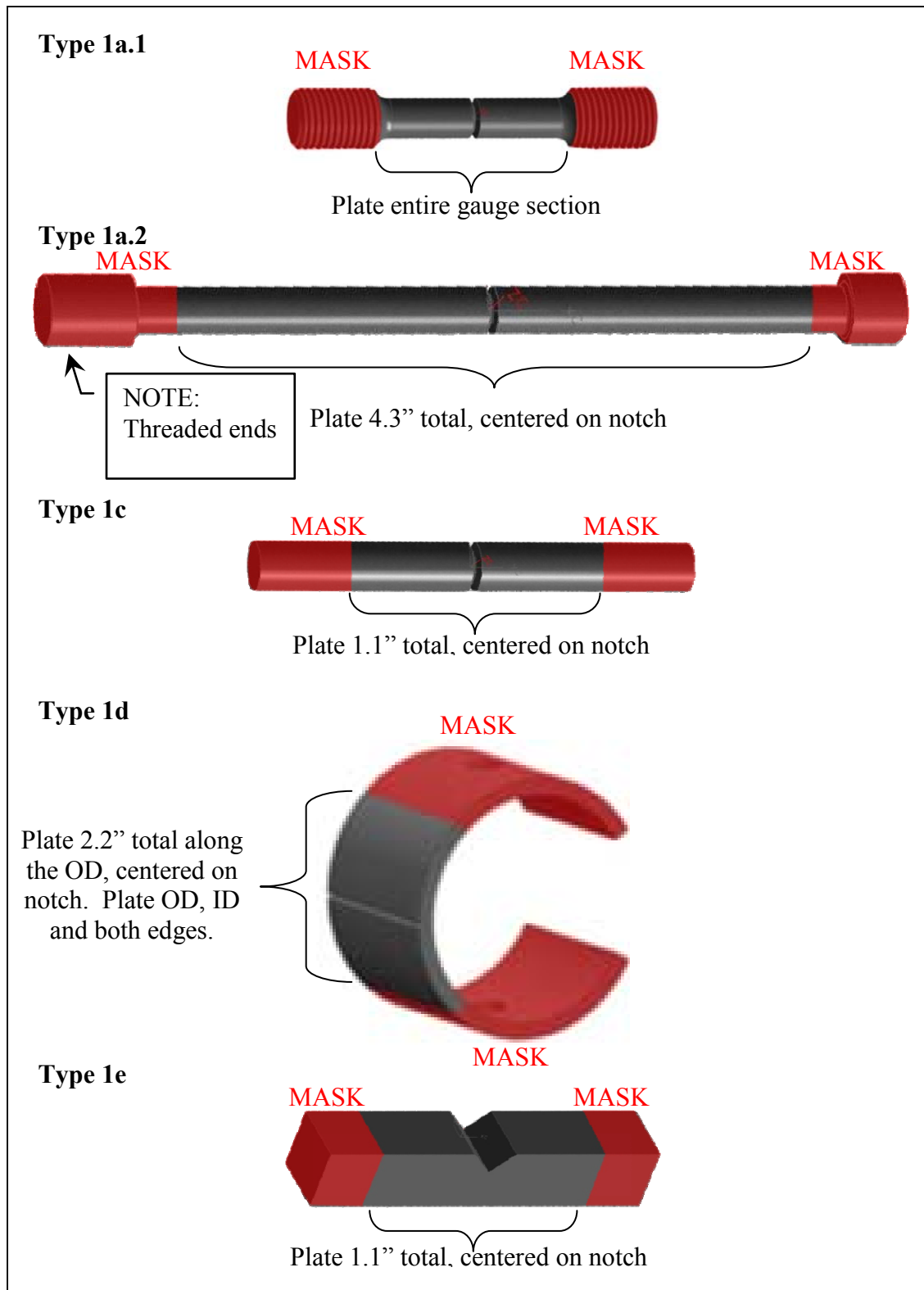


Figure 2. Masking/plating of the five specimen geometries.

4. Experimental Procedures

4.1 DoE

This approach was used over a range of material strength for air-melted grade 4340 steel, load level, and hydrogen environment. The five geometries were tested while load levels were monitored to determine a precise time to fracture at specific percentages of notch fracture strength (NFS), specific material strengths (heat treat tempers T1-T5), and specific hydrogen emitting environment (sodium chloride weight-percent NaCl). Conversely to the existing standard, greater information was gleaned beyond the result of a pass/fail test. By incorporating the failure time, load, and stress level data into DoE failure models, predictive equations over the broad ranges were developed.

The DoE focused on three variables for the five geometries (ASTM-F-519 types 1a.1, 1a.2, 1c, 1d, and 1e). The control variables were selected from risk reduction and ruggedness leveraged efforts conducted by The Boeing Company with the assistance of ARL. The five geometries were selected from the ASTM-F-519 test method. Table 2 presents the range of test conditions for the five ASTM-F-519 test geometries researched.

Table 2. Design of experiment conditions matrix.

Condition	$-\alpha$	–	0	+	$+\alpha$
Strength (ksi)	140	158	210	262	280
Test Load (% NFS)	40	45	60	75	95
NaCl Concentration (weight-percent NaCl)	1.25E-05	0.01	0.50	2.36	3.5

Below 140 ksi steel is generally accepted as not being sensitive to hydrogen, which set the lower limit for strength. NaCl was not used at 0%, essentially completely de-ionized water, since the working group had experience that de-ionized water is actually severely corrosive and a very harsh environment for steel. It is also not a real world environment.

The design of experiment approach was refined with preliminary ruggedness and risk reduction efforts at Boeing Mesa, with technical assistance from Boeing St. Louis, Seattle, and the U.S. Army Research Laboratory (ARL). Typical of DoEs, it consisted of three test portions, a linear portion, a quadratic portion, and a confirmation portion. The example matrix is as presented in tables 3 through 5 with the condition values corresponding to table 2. These experiments aided the development of appropriate boundary conditions for the larger effort.

Table 3. Linear portion test matrix.

		A	B	C	Run Order
Repeat entire matrix 2× for 1a.1, 1a.2, 1c, 1d and 1e	RUN ID	Strength (ksi)	Test Load (%NFS)	NaCl Conc. (weight-percent NaCl)	
Linear Portion	L1	–	–	–	Random
	L2	–	–	+	
	L3	–	+	–	
	L4	–	+	+	
	L5	+	–	–	
	L6	+	–	+	
	L7	+	+	–	
	L8	+	+	+	
Center Points	C1	0	0	0	
	C2	0	0	0	
	C3	0	0	0	
	C4	0	0	0	
	C5	0	0	0	
	C6	0	0	0	

Table 4. Quadratic portion test matrix.

		A	B	C	Run Order
Repeat Q1–Q6 5× for 1a.1, 1a.2, 1c, 1d and 1e	RUN ID	Strength (ksi)	Test Load (%NFS)	NaCl Conc. (weight-percent NaCl)	
Not Replicated	C7	0	0	0	First
Quadratic Portion	Q1	$+\alpha$	0	0	Random
	Q2	$-\alpha$	0	0	
	Q3	0	$+\alpha$	0	
	Q4	0	$-\alpha$	0	
	Q5	0	0	$+\alpha$	
	Q6	0	0	$-\alpha$	
Not Replicated	C8	0	0	0	Last

Table 5. Confirmation portion test matrix.

		A	B	C	
	RUN ID	Strength (ksi)	Test Load (%NFS)	NaCl Conc. (weight-percent NaCl)	Run Order
Confirmation Portion	1	Varied depending on outcome of linear, center, and quadratic			Random
	2				
	3				
	4				
	5				
	6				
	7				
	8				
	9				
	10				
	11				
	12				
	13				
	14				
	15				
	16				

After the linear and center point data runs are completed, initial calculations were made for the predictive model equations. Those initial models were utilized to choose confirmation runs to be researched. The confirmation run results were then incorporated into refining the initial working model.

4.2 Specimens, Environments, and Loading Procedure

Air-melted 4340 steel samples in five ASTM-F-519 geometries and heat treated to five different material strengths, as previously described, were tested. The specimens demonstrated adequate hydrogen sensitivity of the material conducted in accordance with ASTM-F-519.⁵ The cadmium plated specimens used for these experiments are depicted in figure 3. The axially loaded specimens (geometries 1a.1 and 1a.2) were tested on Instron or MTS uniaxial load mechanical test frames; the 1c and 1e specimens were loaded with double cantilever bending fixtures; and the 1d specimens were directly loaded with nut and bolt. The loads were monitored with the load cells on the mechanical test frames and via loading rings installed in the load path for the other geometries. The load cells and load rings were calibrated prior to the experiments. For

⁵ Ibid, page 1.

this work, loads were applied as a percentage (45%–95%) of the calculated 100% NFS determined for each geometry. Ten specimens were utilized to calculate the average 100% NFS with the identical fixturing applied during the experiments. Ten specimens from each group were loaded to failure. The experimental loading was then applied as a percentage of this determined average NFS failure load. Loads were recorded from the mechanical test frames for geometries 1a1 and 1a.2, and with data sampling hardware and software for the other geometries. Figures 4 through 7 depict the in-situ test apparatus for the experiments.

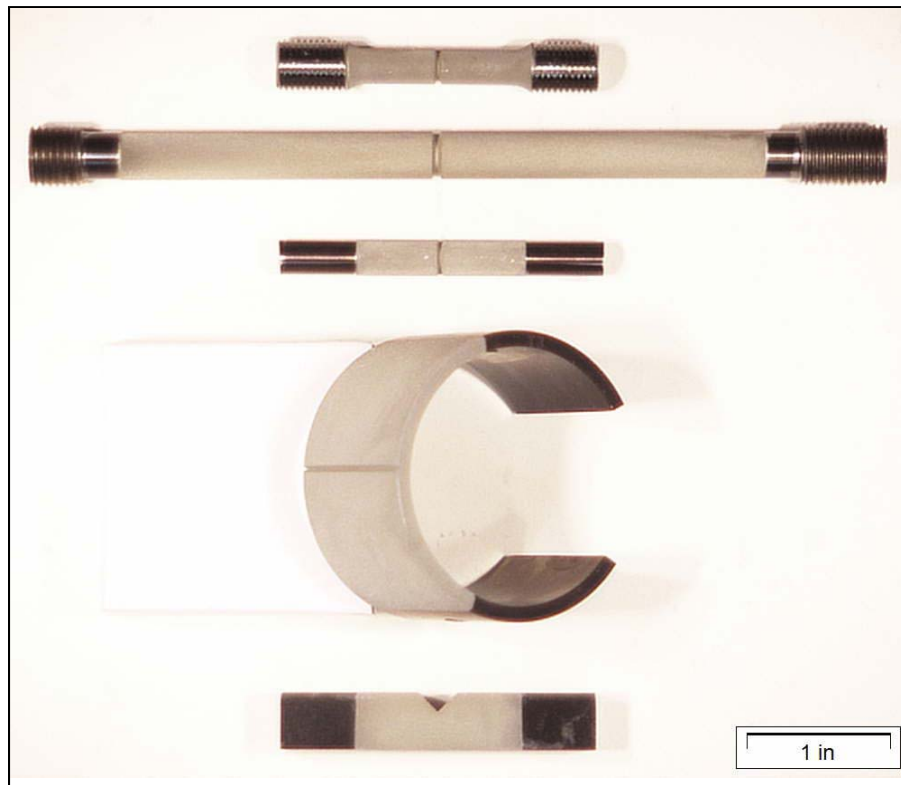


Figure 3. Cadmium plated experimental specimens (top to bottom; 1a.1, 1a.2, 1c, 1d, and 1e).

The samples were cadmium plated at Asko Processing, Inc., Seattle, WA in accordance with MIL-STD-870 Rev. C. Type II, Class 1.⁶ Plated samples were sensitivity tested in accordance with ASTM-F-519.⁷ Cadmium plating process embrittlement testing involved loading three T5 samples from each geometry to 75% of their NFS and holding for 200 h in air. These specimens did not fail, and thus insured that the plating process did not embrittle the specimens.

⁶ Ibid, page 1.

⁷ Ibid, page 1.

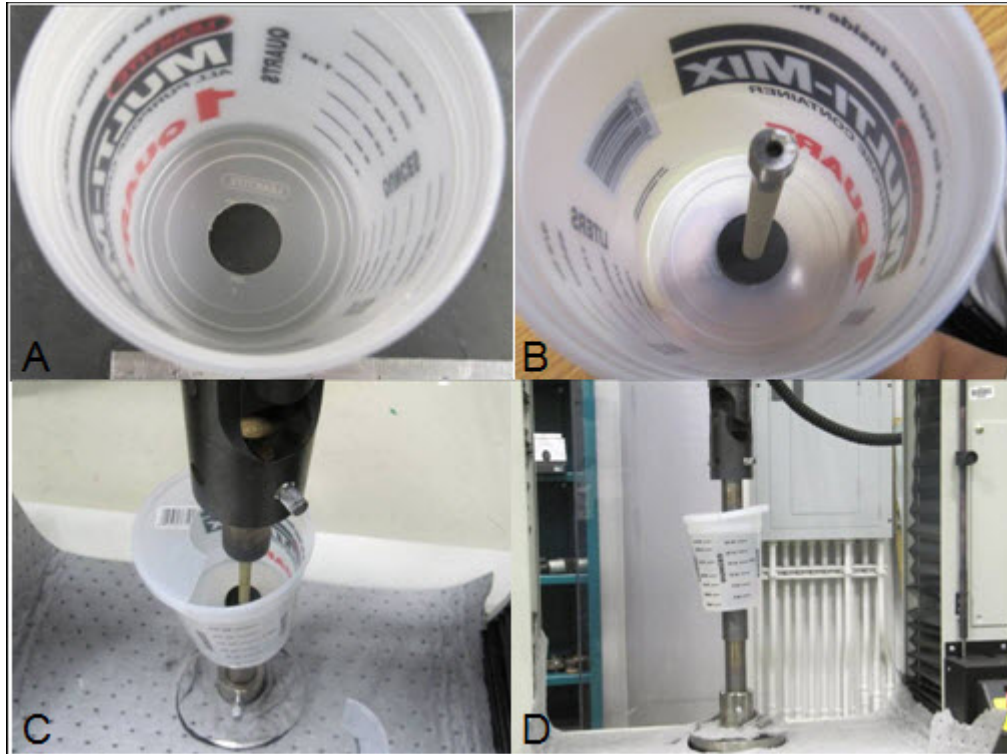


Figure 4. Geometry 1a.1 and 1a.2 in-situ environmental setup. A) the empty container, B) the sample in the cup, C) the sample loaded onto the mechanical test frame, and D) the sample being tested in solution.

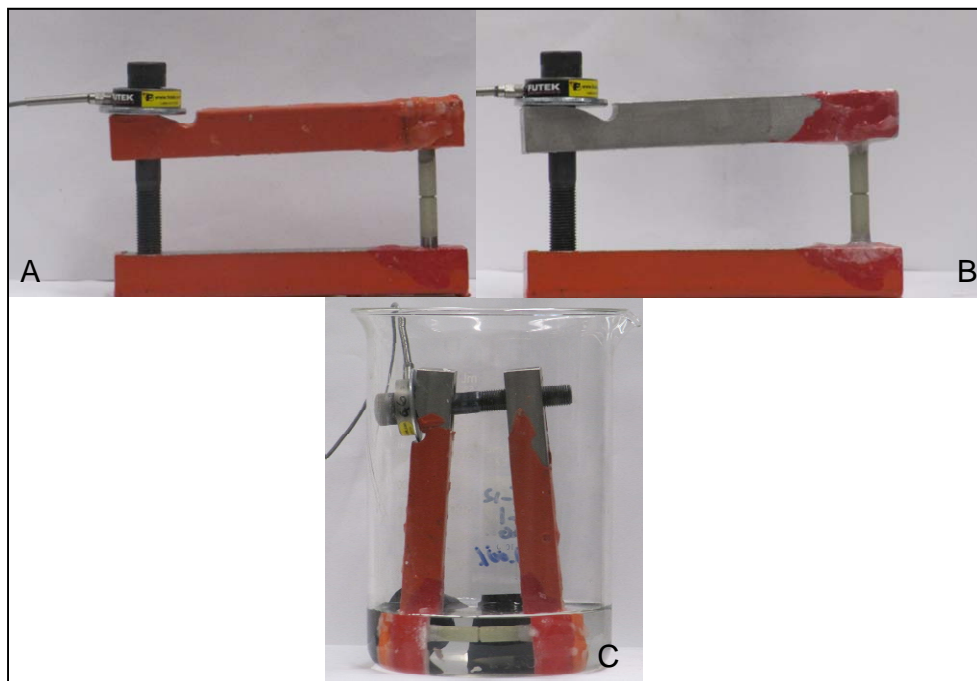


Figure 5. Geometry 1c in-situ environmental setup. A) loaded, B) loaded and masked, and C) being tested in solution.

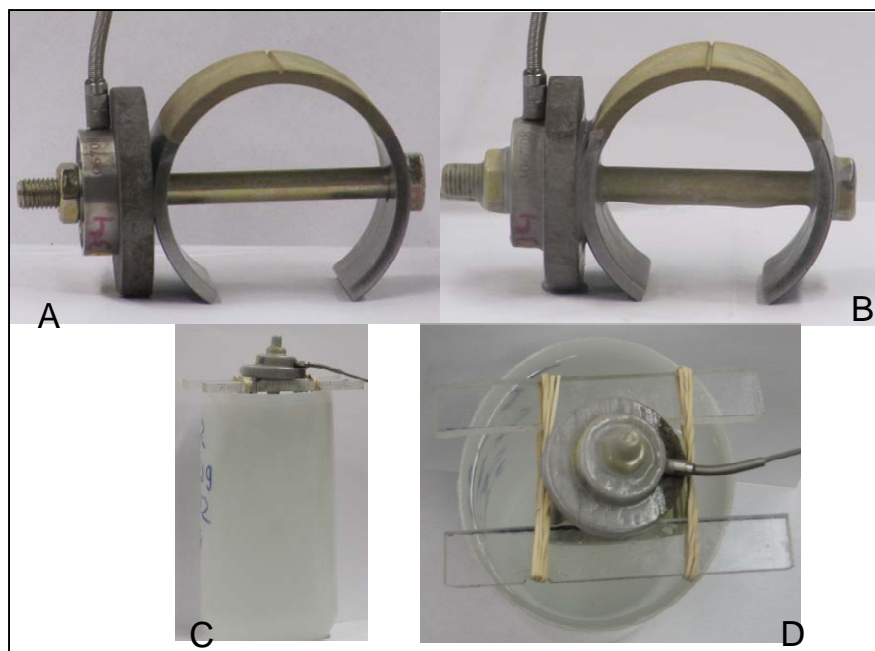


Figure 6. Geometry 1d in-situ environmental setup. A) loaded, B) loaded and masked, C) being tested in solution, and D) top-down perspective.

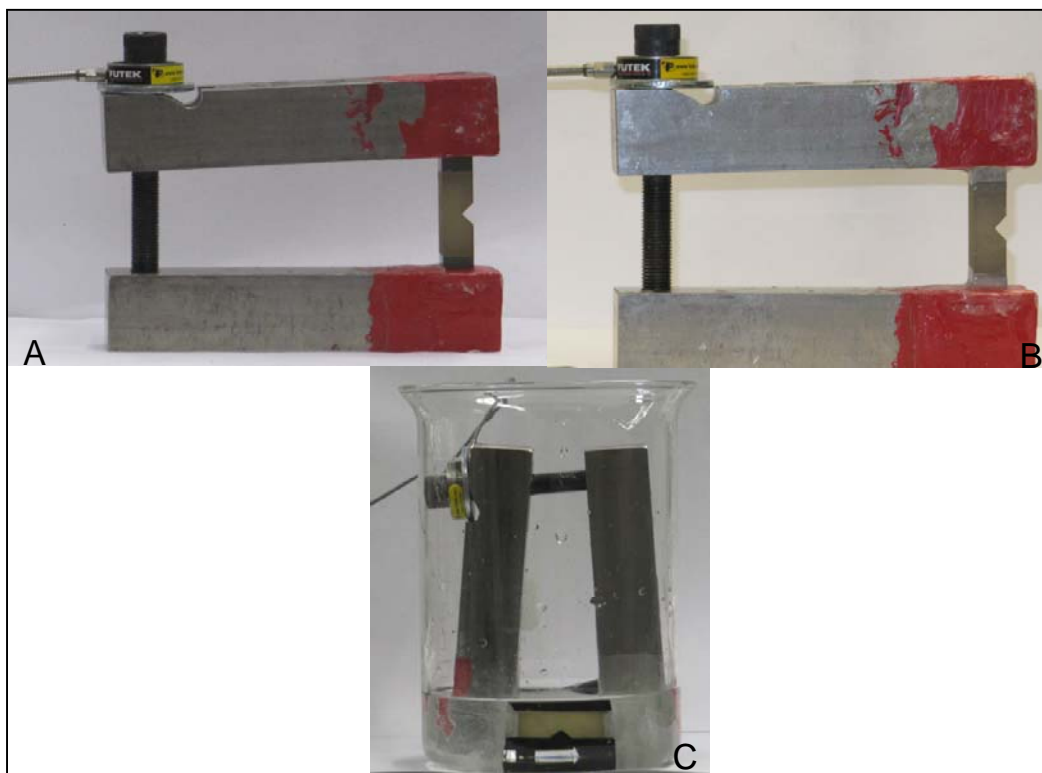


Figure 7. Geometry 1e in-situ environmental setup. A) loaded, B) loaded and masked, and C) being tested in salt water.

The specimens were masked so that only the cadmium plated surface contacted the test solution. The solution used was NaCl in de-ionized water in five different concentrations; 1.25e-5 weight-percent, 0.01 weight-percent, 0.5 weight-percent, 2.36 weight-percent, and 3.5 weight-percent in accordance with table 2. The volume of NaCl solution for each sample geometry was calculated to ensure that each geometry had the same ratio of cadmium plated surface area to solution volume (if this volume was not enough to submerge the samples adequately, clean inert material was added to displace solution in order to submerge the samples to the correct level.) The loaded specimens were then immersed in the test solution for the duration of the experiment. Specimens were removed either upon failure or after 168 h of sustained load without failure. The result of each individual test run for each geometry can be found in the appendices.

As stated previously, upon conclusion of the linear, center and quadratic test runs preliminary life prediction models were created. These models were then used in the confirmation test portion of the matrix to choose appropriate parameters to both enhance and verify the model. Final life prediction equations and three dimensional models were created after the incorporation of the confirmation data.

5. Results

The raw test experimental data is presented in the appendices. The following sections and tables 6 through 15 present the preliminary and final model equations and parameter analyses for each geometry. The final graphical life prediction model for each geometry is shown in figures 8 through 12 for type 1a.1, 1a.2, 1c, 1d, and 1e, respectively. The final life prediction models, for each respective geometry, did not vary significantly from the preliminary set, thus verifying the initial prediction. The variables in the models are material strength, test load and NaCl concentration. The model transformations of these variables were as follows:

$$Str = \frac{Material\ Strength\ (in\ ksi) - 210}{52} \quad (1)$$

$$Load = (Test\ Load\ (in\ \% \ of\ NFS) \times 0.0444) - 3.2222 \quad (2)$$

$$NaCl = (NaCl\ concentration\ \%)^{\frac{1}{3}} \times 1.782 - 1.376 \quad (3)$$

1a.1 Preliminary Model:

$$\ln(T) = 7.20 - 5.09 \cdot \text{Str} - 2.43 \cdot \text{Load} - 1.02 \cdot \text{NaCl} - 2.43 \cdot \text{Str} \cdot \text{Load} + \text{Offset} \quad (4)$$

where

$$\text{Offset} = \sigma \times \ln(-\ln(1 - P))$$

for which

T = time to event. It is either the time to failure or the time to the end of the experiment (168 hrs).

P = the predicted percentile. At a P of 70%, 70% of the failures would be above the curve and 30% would fall below the curve generated.

σ = 1/Weibull shape parameter.

Note: Weibull shape parameter = 0.5787

- A negative value of the coefficient is indicative of shorter lifetime as the variable increases.
- Weibull shape $< 1 \rightarrow$ hazard rate (failure rate) decreases as time increases.
- Infant mortality: after initial early failures the survival gets better with age.

1a.1 Confirmation Model:

$$\ln(T) = 6.77 - 4.98 \cdot \text{Str} - 1.29 \cdot \text{Load} - 0.93 \cdot \text{NaCl} - 3.66 \cdot \text{Str} \cdot \text{Load} + \text{Offset} \quad (5)$$

where

$$\text{Offset} = \sigma \times \ln(-\ln(1 - P))$$

for which

T = time to event. It is either the time to failure or the time to the end of the experiment (168 hrs).

P = the predicted percentile. At a P of 70%, 70% of the failures would be above the curve and 30% would fall below the curve generated.

σ = 1/Weibull shape parameter.

Note: Weibull shape parameter = 0.567

- A negative value of the coefficient is indicative of shorter lifetime as the variable increases.
- Weibull shape < 1 → hazard rate (failure rate) decreases as time increases.
- Infant mortality: after initial early failures the survival gets better with age.

Table 6. Preliminary 1a.1 equation parameter analysis estimates.

Parameter	DF	Estimate	Standard Error	95% Confidence Limits		Chi-Square	Pr > ChiSq
Intercept	1	7.1994	1.0512	5.1391	9.2598	46.90	<0.0001
Strength	1	-5.0906	1.1559	-7.3561	-2.8250	19.39	<0.0001
Test_load	1	-2.4281	1.4911	-5.3506	0.4944	2.65	0.1034
Nacl_conc	1	-1.0160	0.4964	-1.9890	-0.0430	4.19	0.0407
Strength*test_load	1	-2.4345	1.6662	-5.7003	0.8313	2.13	0.1440
Weibull shape	1	0.5787	0.0993	0.4134	0.8099	—	—

Table 7. Final 1a.1 equation parameter analysis estimates.

Parameter	DF	Estimate	Standard Error	95% Confidence Limits		Chi-Square	Pr > ChiSq
Intercept	1	6.7672	0.9415	4.9219	8.6125	51.66	<0.0001
Strength	1	-4.9801	1.0506	-7.0392	-2.9210	22.47	<0.0001
Test_load	1	-1.2892	1.3813	-3.9965	1.4182	0.87	0.3507
Nacl_conc	1	-0.9282	0.4518	-1.8137	-0.0427	4.22	0.0399
Strength*test_load	1	-3.6568	1.4358	-6.4710	-0.8427	6.49	0.0109
Weibull shape	1	0.5666	0.0899	0.4152	0.7731	—	—

1a.2 Preliminary Model:

$$\ln(T) = 9.09 - 5.49 \cdot \text{Str} - 7.39 \cdot \text{Load} - 1.39 \cdot \text{NaCl} + \text{Offset} \quad (6)$$

where

$$\text{Offset} = \sigma \times \ln(-\ln(1 - P))$$

for which

T = time to event. It is either the time to failure or the time to the end of the experiment (168 hrs).

P = the predicted percentile. At a P of 70%, 70% of the failures would be above the curve and 30% would fall below the curve generated.

$\sigma = 1/\text{Weibull shape parameter}$.

Note: Weibull shape parameter = 0.377

- A negative value of the coefficient is indicative of shorter lifetime as the variable increases.
- Weibull shape < 1 → hazard rate (failure rate) decreases as time increases.
- Infant mortality: after initial early failures the survival gets better with age.

1a.2 Confirmation Model:

$$\ln(T) = 8.75 - 5.90 \cdot \text{Str} - 6.53 \cdot \text{Load} - 1.33 \cdot \text{NaCl} + \text{Offset} \quad (7)$$

where

$$\text{Offset} = \sigma \times \ln(-\ln(1 - P))$$

for which

T = time to event. It is either the time to failure or the time to the end of the experiment (168 hrs).

P = the predicted percentile. At a P of 70%, 70% of the failures would be above the curve and 30% would fall below the curve generated.

$\sigma = 1/\text{Weibull shape parameter}$.

Note: Weibull shape parameter = 0.397

- A negative value of the coefficient is indicative of shorter lifetime as the variable increases.
- Weibull shape < 1 → hazard rate (failure rate) decreases as time increases.
- Infant mortality: after initial early failures the survival gets better with age.

Table 8. Preliminary 1a.2 equation parameter analysis estimates.

Parameter	DF	Estimate	Standard Error	95% Confidence Limits		Chi-Square	Pr > ChiSq
Intercept	1	9.0934	1.0318	7.0711	11.1157	77.67	<0.0001
Strength	1	-5.4866	0.8532	-7.1589	-3.8144	41.35	<0.0001
Test_load	1	-7.3903	1.4996	-10.3296	-4.4511	24.29	<0.0001
Nacl_conc	1	-1.3858	0.5576	-2.4786	-0.2929	6.18	0.0129
Weibull shape	1	0.3769	0.0568	0.2805	0.5064	—	—

Table 9. Final 1a.2 equation parameter analysis estimates.

Parameter	DF	Estimate	Standard Error	95% Confidence Limits		Chi-Square	Pr > ChiSq
Intercept	1	8.7526	0.8021	7.1805	10.3247	119.07	<0.0001
Strength	1	-5.9048	0.7752	-7.4242	-4.3854	58.02	<0.0001
Test_load	1	-6.5283	1.1046	-8.6933	-4.3634	34.93	<0.0001
Nacl_conc	1	-1.3309	0.4556	-2.2239	-0.4379	8.53	0.0035
Weibull shape	1	0.3965	0.0542	0.3033	0.5184	—	—

1c Preliminary Model:

$$\ln(T) = 19.01 - 11.67 \cdot \text{Str} - 9.93 \cdot \text{Load} - 0.88 \cdot \text{NaCl} + \text{Offset} \quad (8)$$

where

$$\text{Offset} = \sigma \times \ln(-\ln(1 - P))$$

for which

T = time to event. It is either the time to failure or the time to the end of the experiment (168 hrs).

P = the predicted percentile. At a P of 70%, 70% of the failures would be above the curve and 30% would fall below the curve generated.

$\sigma = 1/\text{Weibull shape parameter}$.

Note: Weibull shape parameter = 0.343

- A negative value of the coefficient is indicative of shorter lifetime as the variable increases.
- Weibull shape < 1 → hazard rate (failure rate) decreases as time increases.
- Infant mortality: after initial early failures the survival gets better with age.

1c Confirmation Model:

$$\ln(T) = 20.91 - 10.53 \cdot \text{Str} - 11.30 \cdot \text{Load} - 1.25 \cdot \text{NaCl} + \text{Offset} \quad (9)$$

where

$$\text{Offset} = \sigma \times \ln(-\ln(1 - P))$$

for which

T = time to event. It is either the time to failure or the time to the end of the experiment (168 hrs).

P = the predicted percentile. At a P of 70%, 70% of the failures would be above the curve and 30% would fall below the curve generated.

σ = 1/Weibull shape parameter.

Note: Weibull shape parameter = 0.278

- A negative value of the coefficient is indicative of shorter lifetime as the variable increases.
- Weibull shape < 1 \rightarrow hazard rate (failure rate) decreases as time increases.
- Infant mortality: after initial early failures the survival gets better with age.

Table 10. Preliminary 1c equation parameter analysis estimates.

Parameter	DF	Estimate	Standard Error	95% Confidence Limits		Chi-Square	Pr > ChiSq
Intercept	1	19.0121	3.9863	11.1990	26.8252	22.75	<0.0001
Strength	1	-11.6674	2.8531	-17.2594	-6.0755	16.72	<0.0001
Test_load	1	-9.9313	2.8949	-15.6052	-4.2573	11.77	0.0006
Nacl_conc	1	-0.8804	1.0752	-2.9877	1.2269	0.67	0.4129
Weibull shape	1	0.3434	0.0949	0.1998	0.5902	—	—

Table 11. Final 1c equation parameter analysis estimates.

Parameter	DF	Estimate	Standard Error	95% Confidence Limits		Chi-Square	Pr > ChiSq
Intercept	1	20.9051	4.6112	11.8673	29.9429	20.55	<0.0001
Strength	1	-10.5250	2.8420	-16.0953	-4.9547	13.71	0.0002
Test_load	1	-11.3049	4.0160	-19.1761	-3.4337	7.92	0.0049
Nacl_conc	1	-1.2535	1.0574	-3.3259	0.8189	1.41	0.2358
Weibull shape	1	0.2784	0.0642	0.1772	0.4375	—	—

1d Preliminary Model:

$$\ln(T) = 7.83 - 4.04 \cdot \text{Str} - 3.54 \cdot \text{Load} - 1.01 \cdot \text{NaCl} + \text{Offset} \quad (10)$$

where

$$\text{Offset} = \sigma \times \ln(-\ln(1 - P))$$

for which

T = time to event. It is either the time to failure or the time to the end of the experiment (168 hrs).

P = the predicted percentile. At a P of 70%, 70% of the failures would be above the curve and 30% would fall below the curve generated.

σ = 1/Weibull shape parameter.

Note: Weibull shape parameter = 0.515

- A negative value of the coefficient is indicative of shorter lifetime as the variable increases.
- Weibull shape < 1 → hazard rate (failure rate) decreases as time increases.
- Infant mortality: after initial early failures the survival gets better with age.

1d Confirmation Model:

$$\ln(T) = 7.68 - 4.12 \cdot \text{Str} - 3.08 \cdot \text{Load} - 6.04 \cdot \text{NaCl} + \text{Offset} \quad (11)$$

where

$$\text{Offset} = \sigma \times \ln(-\ln(1 - P))$$

for which

T = time to event. It is either the time to failure or the time to the end of the experiment (168 hrs).

P = the predicted percentile. At a P of 70%, 70% of the failures would be above the curve and 30% would fall below the curve generated.

$\sigma = 1/\text{Weibull shape parameter}$.

Note: Weibull shape parameter = 0.546

- A negative value of the coefficient is indicative of shorter lifetime as the variable increases.
- Weibull shape < 1 → hazard rate (failure rate) decreases as time increases.
- Infant mortality: after initial early failures the survival gets better with age.

Table 12. Preliminary 1d equation parameter analysis estimates.

Parameter	DF	Estimate	Standard Error	95% Confidence Limits		Chi-Square	Pr > ChiSq
Intercept	1	7.8301	0.7829	6.2956	9.3645	100.03	<0.0001
Strength	1	-4.0458	0.7147	-5.4466	-2.6451	32.05	<0.0001
Test load	1	-3.5487	1.0095	-5.5273	-1.5700	12.36	0.0004
Nacl_conc	1	-1.0116	0.5366	-2.0634	0.0402	3.55	0.0594
Weibull shape	1	0.5151	0.0809	0.3786	0.7008	—	—

Table 13. Final 1d equation parameter analysis estimates.

Parameter	DF	Estimate	Standard Error	95% Confidence Limits		Chi-Square	Pr > ChiSq
Intercept	1	7.6813	0.6130	6.4798	8.8828	157.00	<0.0001
Strength	1	-4.1169	0.6567	-5.4041	-2.8298	39.30	<0.0001
Test_load	1	-3.0758	0.7160	-4.4792	-1.6724	18.45	<0.0001
NaCl_conc	1	-0.6044	0.4262	-1.4397	0.2308	2.01	0.1561
Weibull shape	1	0.5459	0.0807	0.4085	0.7294	—	—

1e Preliminary Model:

$$\ln(T) = 12.31 - 7.45 \cdot \text{Str} - 6.45 \cdot \text{Load} - 0.97 \cdot \text{NaCl} + \text{Offset} \quad (12)$$

where

$$\text{Offset} = \sigma \times \ln(-\ln(1 - P))$$

for which

T = time to event. It is either the time to failure or the time to the end of the experiment (168 hrs).

P = the predicted percentile. At a P of 70%, 70% of the failures would be above the curve and 30% would fall below the curve generated.

$\sigma = 1/\text{Weibull shape parameter}$.

Note: Weibull shape parameter = 0.505

- A negative value of the coefficient is indicative of shorter lifetime as the variable increases.
- Weibull shape < 1 → hazard rate (failure rate) decreases as time increases.
- Infant mortality: after initial early failures the survival gets better with age.

1e Confirmation Model:

$$\ln(T) = 13.14 - 8.16 \cdot \text{Str} - 6.58 \cdot \text{Load} - 0.73 \cdot \text{NaCl} + \text{Offset} \quad (13)$$

where

$$\text{Offset} = \sigma \times \ln(-\ln(1 - P))$$

for which

T = time to event. It is either the time to failure or the time to the end of the experiment (168 hrs).

P = the predicted percentile. At a P of 70%, 70% of the failures would be above the curve and 30% would fall below the curve generated.

$\sigma = 1/\text{Weibull shape parameter}$.

Note: Weibull shape parameter = 0.493

- A negative value of the coefficient is indicative of shorter lifetime as the variable increases.
- Weibull shape $< 1 \rightarrow$ hazard rate (failure rate) decreases as time increases.
- Infant mortality: after initial early failures the survival gets better with age

Table 14. Preliminary 1e equation parameter analysis estimates.

Parameter	DF	Estimate	Standard Error	95% Confidence Limits		Chi-Square	Pr > ChiSq
Intercept	1	12.3119	1.5789	9.2174	15.4065	60.81	<0.0001
Strength	1	-7.4452	1.2525	-9.9000	-4.9904	35.34	<0.0001
Test_load	1	-6.4528	1.4027	-9.2020	-3.7037	21.16	<0.0001
Nacl_conc	1	-0.9682	0.7589	-2.4557	0.5192	1.63	0.2020
Weibull shape	1	0.5048	0.1063	0.3341	0.7626	—	—

Table 15. Final 1e equation parameter analysis estimates.

Parameter	DF	Estimate	Standard Error	95% Confidence Limits		Chi-Square	Pr > ChiSq
Intercept	1	13.1443	1.5765	10.0545	16.2341	69.52	<0.0001
Strength	1	-8.1572	1.2984	-10.7019	-5.6124	39.47	<0.0001
Test_load	1	-6.5768	1.3150	-9.1541	-3.9996	25.02	<0.0001
Nacl_conc	1	-0.7324	0.6134	-1.9347	0.4699	1.43	0.2325
Weibull shape	1	0.4933	0.0955	0.3375	0.7210	—	—

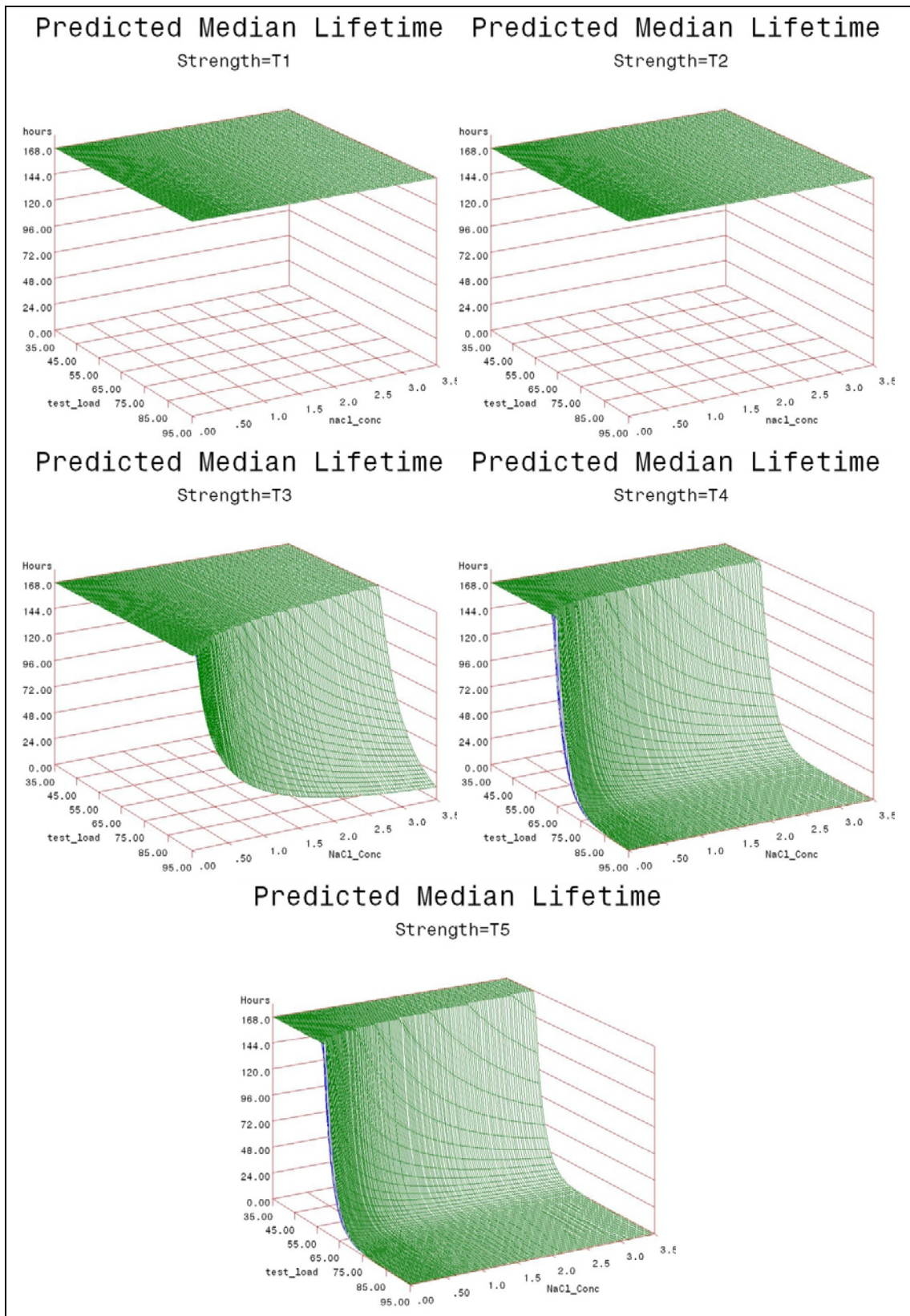


Figure 8. Final 1a.1 specimen geometry life prediction models.

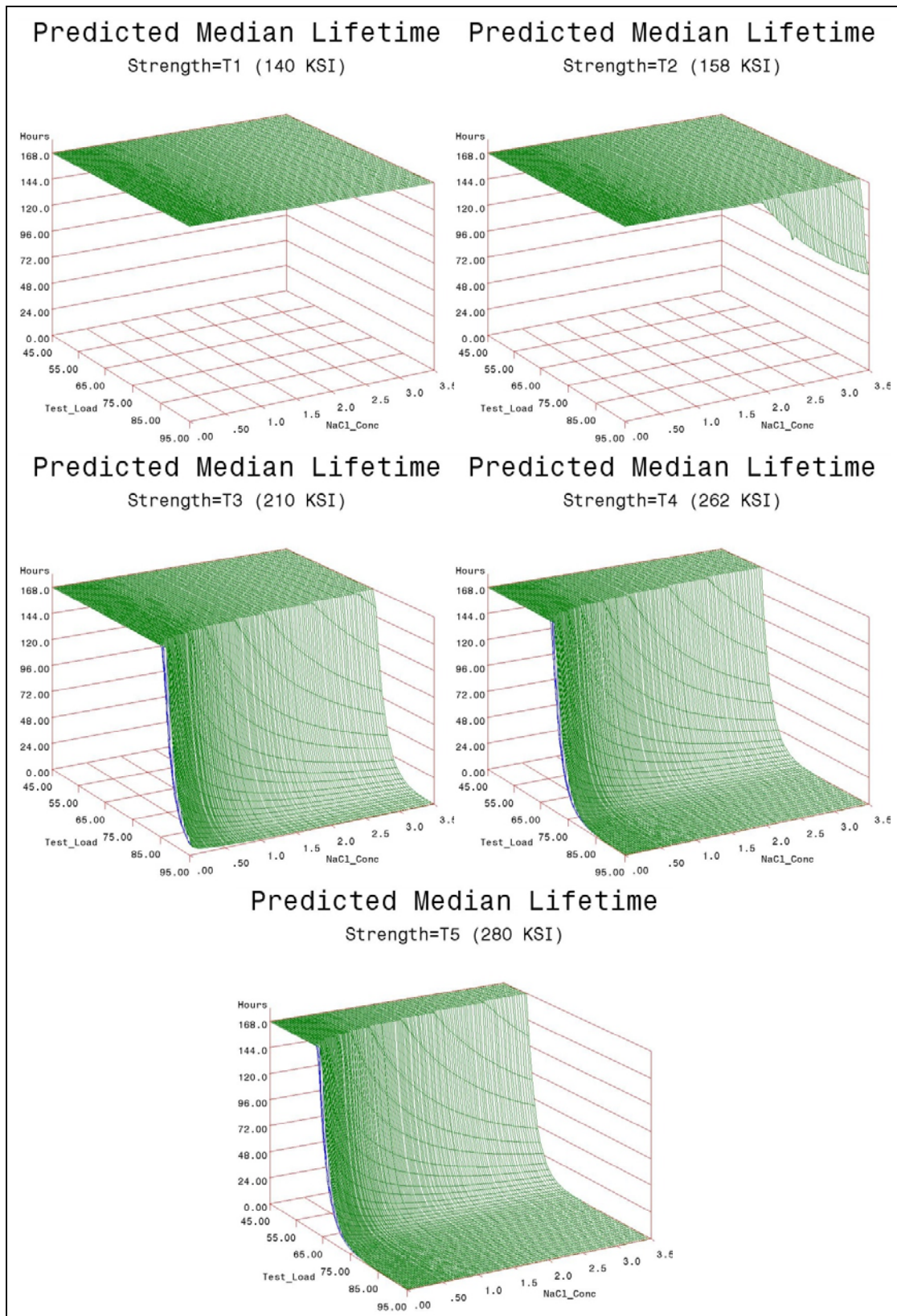


Figure 9. Final 1a.2 specimen geometry life prediction models.

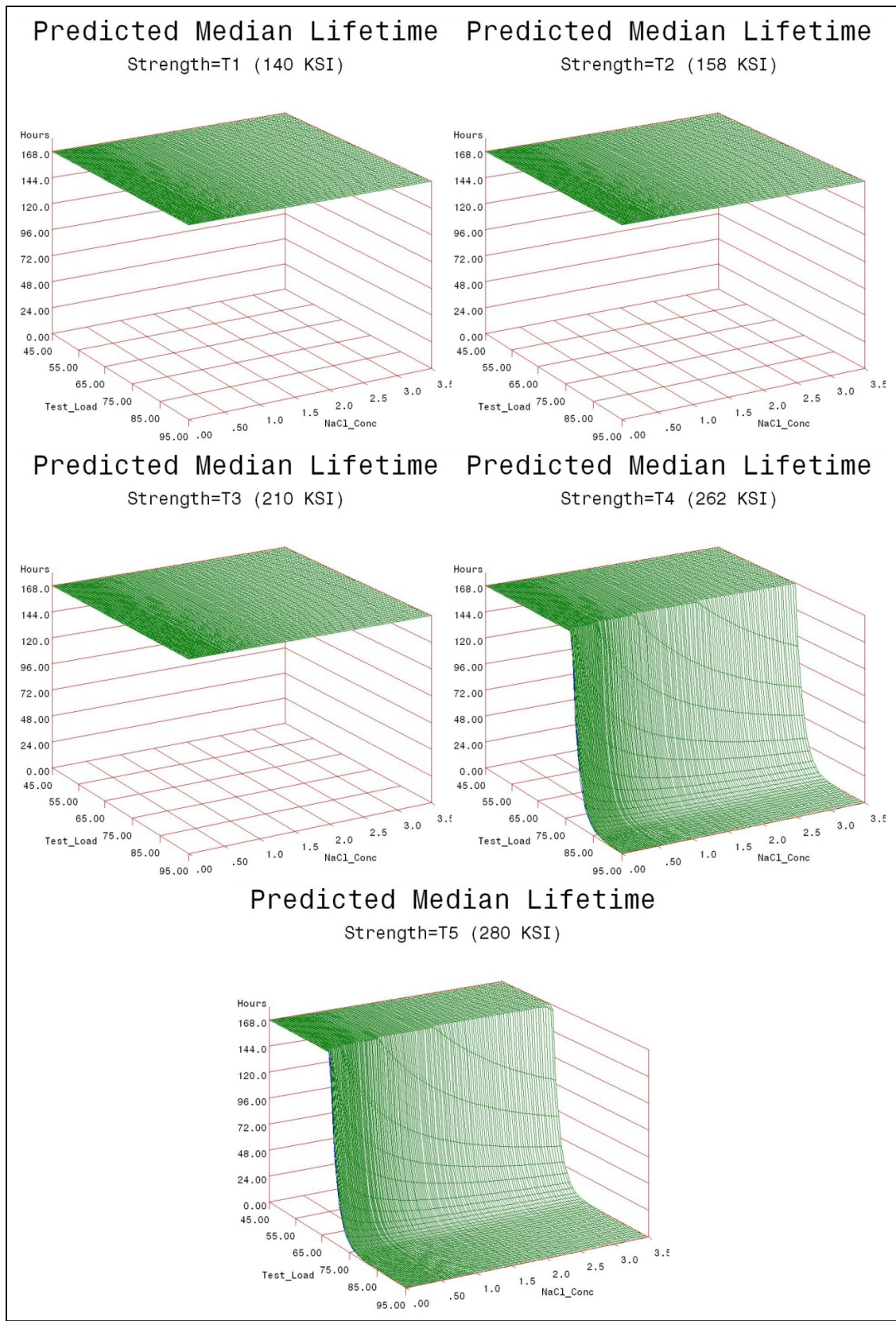


Figure 10. Final 1c specimen geometry life prediction models.

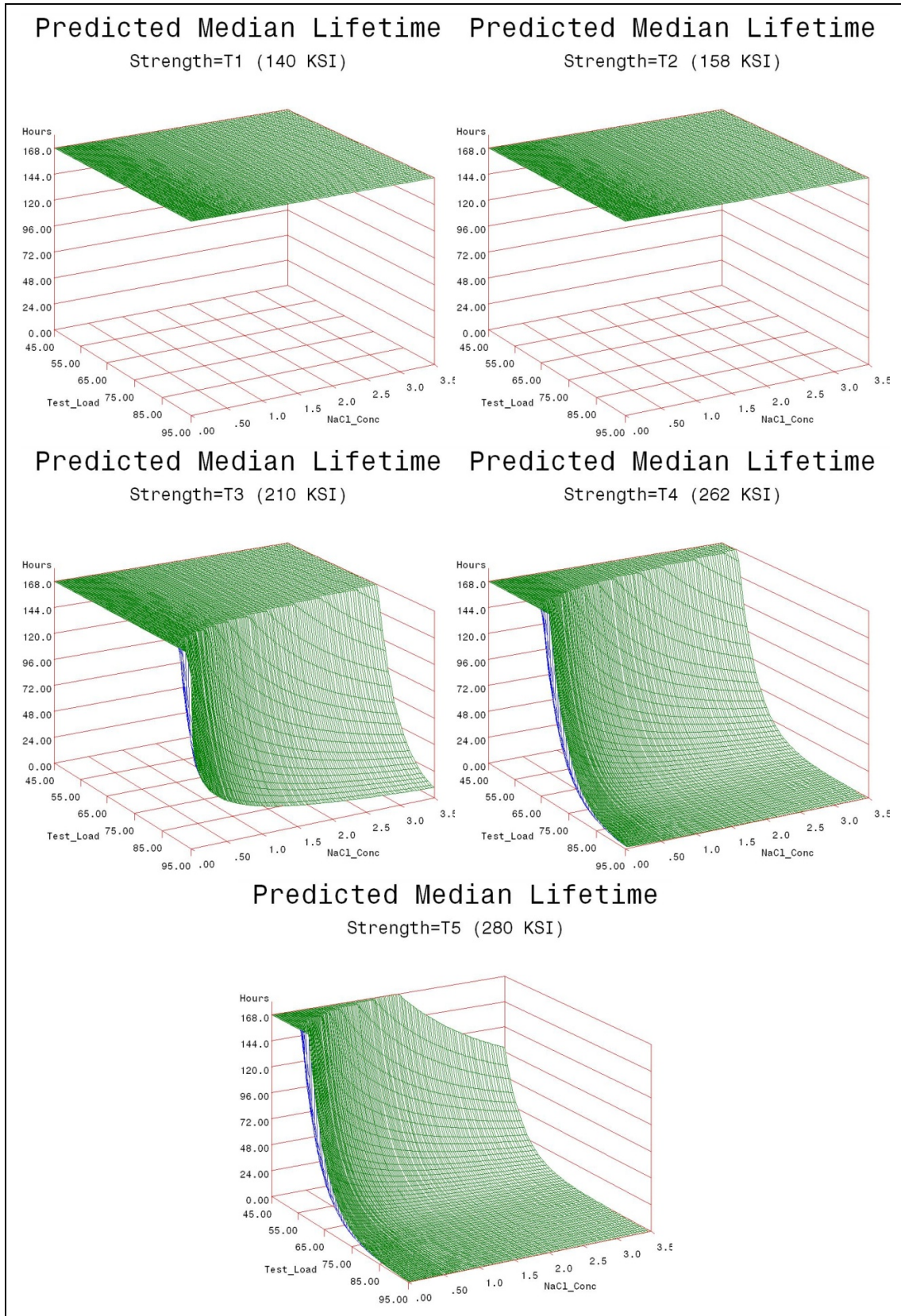


Figure 11. Final 1d specimen geometry life prediction models.

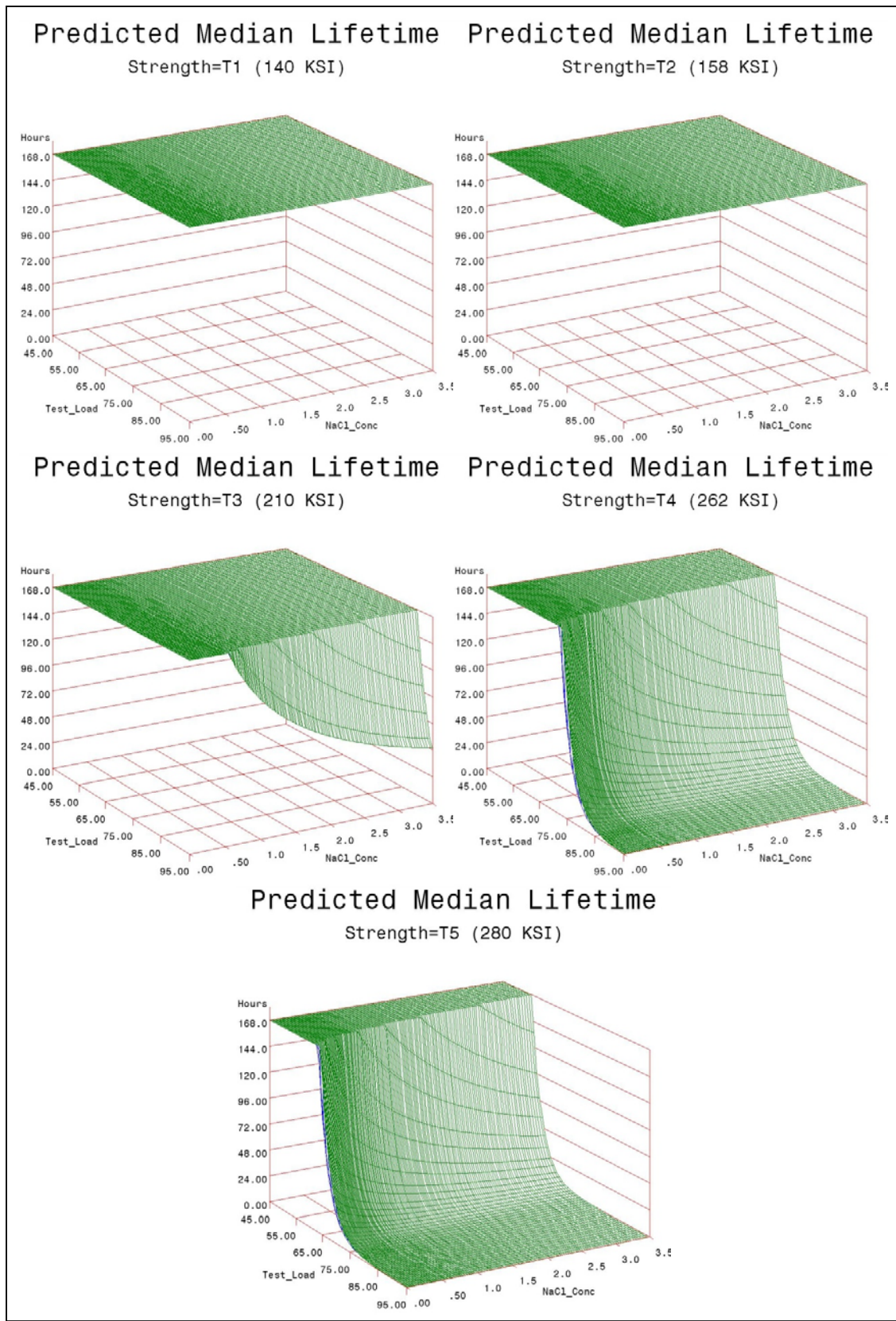


Figure 12. Final 1e specimen geometry life prediction models.

6. Discussion

Since this type of predictive model had never been attempted before to assess hydrogen sensitivity, the results were extremely satisfying. The predictive models express hydrogen sensitivity in terms of applied load, material strength and hydrogen environment. In this case, the hydrogen environment is a representation of the natural environmental corrosion cycle. In terms of NaCl salt concentration, 3.5% is widely accepted to be the worst case scenario for corrosion of steel. Values higher than 3.5% actually result in a lower corrosion rate. The time duration, 168 h, is above that which is accepted as the lifetime cutoff for service environments, 150 h. Essentially, this data suggests that if the material demonstrates no hydrogen sensitivity in a 3.5% salt concentration environment for 168 h at a specific strength and applied load combination, then it should not be expected to fail in a lifetime of service exposure in our natural environment at that strength and applied load level. The “safe zone” in the graphical representation of the models is the area below the curves.

By comparing all of the models across test geometry, it can be seen that the 3.5% NaCl is not a severe enough environment to cause hydrogen embrittlement at or below the 158 ksi strength level. The “T1, 140 ksi” and “T2, 158 ksi” strength levels are flat, showing no sensitivity. This does not mean that in an environment that emits more hydrogen, no sensitivity would be expected. The converse is true, industrial processes like electroplating, or acidic or alkaline cleaning would certainly be expected to show sensitivity to hydrogen at or near the 158 ksi material strength level.

Although varying performance can be observed across test geometry, the trends are certainly in agreement. The sensitivity increases with material strength level, applied load, and to a lesser degree, with NaCl concentration. All of these trends are in-line with traditional expectations. While material strength level is typically given consideration with regard to hydrogen sensitivity, applied load is often forgotten. Residual stresses from forming, quenching or from assembly can often reach 40–45% of the UTS. This is important to remember since these life prediction models show sensitivity beginning at or even below that region. This supports traditional findings where components sometimes break on the shelf while waiting to be placed in service. When combined with a design stress or in-service applied stress, catastrophic failure is much more likely to occur. The degree of heightened sensitivity from applied stress was unknown before now, since it has never been investigated.

It can also be observed in the data that the 1d geometry shows the highest sensitivity. It has the highest stress intensity, stemming from the smallest notch root radius. It also has historically performed in comparative tests with heightened sensitivity. While this test geometry may not be representative of every application in terms of stress intensity, one would be able to apply a factor of safety to this life prediction model and have confidence that a similar application would

not fail due to hydrogen embrittlement. All the models have similar trends, but a risk analysis would likely scale from a worst case and not middle of the pack performance. The 1d geometry is also a self loading geometry, so it is conducive to testing in various environments since no mechanical test frame is needed.

7. Conclusions

The following conclusions can be drawn from the data developed within this work:

1. Life prediction models were developed that accurately represent the expected hydrogen sensitivity over the range of parameters explored for air-melted 4340 steel.
2. The trends observed in the data were reasonably consistent across all test geometries. Sensitivity increases with applied load, material strength, and to a lesser degree NaCl concentration.
3. Applied stress has the most direct effect on hydrogen sensitivity, while material strength is a close second. Increasing the value of either parameter directly heightens the sensitivity to hydrogen.
4. Air-melted 4340 steel does not appear susceptible to hydrogen absorbed from environmental corrosion below the 160 ksi strength level.
5. High residual stress levels (40–50% of the ultimate tensile strength, UTS) are capable of causing hydrogen embrittlement without further applied system stresses.
6. The 1d test geometry proved the most sensitive to hydrogen and also conducive to testing multiple specimens in various environments without requiring test load frames.

INTENTIONALLY LEFT BLANK.

Appendix A. 1a.1 Raw Data

This appendix appears in its original form, without editorial change.

Strength	NaCl Conc.	Test Load	TTF
T1	0.5	85	DNF
T1	0.5	90	DNF
T1	0.5	85	DNF
T1	0.5	95	DNF
T1	0.5	95	DNF
T2	0.01	75	DNF
T2	0.01	75	DNF
T2	2.36	85	DNF
T2	2.36	95	DNF
T2	0.01	90	DNF
T2	0.01	95	DNF
T2	2.36	90	DNF
T2	2.36	85	DNF
T2	2.36	95	DNF
T2	0.01	95	DNF
T3	0	75	DNF
T3	0.5	75	6.4
T3	0	75	DNF
T3	0.5	90	DNF
T3	0.5	75	DNF
T3	0.5	90	DNF
T3	3.5	75	112.6
T3	0.5	90	DNF
T3	3.5	75	28.4
T3	0.5	75	DNF
T3	0.5	75	DNF
T3	0.5	60	DNF
T3	0.5	85	DNF
T3	0.5	95	1.1
T3	0	85	DNF
T3	0.5	95	DNF
T3	0.5	85	DNF
T3	0.5	85	138.6
T3	0.5	95	DNF
T3	0.5	85	DNF
T3	0.5	85	28.9
T3	3.5	85	55.4
T3	0	85	2
T3	0.5	85	48.1
T3	0.5	95	1.9
T3	0	85	DNF
T3	3.5	85	7.5
T3	0.5	95	1.6
T3	0.5	85	13.4
T3	0.5	85	DNF
T3	3.5	85	2.4
T3	0.5	85	71.1
T4	0.01	70	47.2
T4	2.36	30	DNF
T4	0.01	30	DNF
T4	2.36	70	11.6
T4	0.01	70	17
T4	0.01	30	DNF
T4	2.36	60	DNF
T4	2.36	80	2.7
T4	2.36	70	0.6
T4	0.01	80	3.6
T5	0.5	70	0.3
T5	0.5	30	DNF
T5	0.5	30	DNF
T5	0.5	70	0.3
T5	0.5	50	46.5
T1	3.5	95	DNF
T2	3.5	95	DNF
T2	2.36	95	DNF
T2	3.5	95	DNF
T2	2.36	95	DNF
T3	0.5	90	DNF
T3	2.36	90	DNF
T4	2.36	65	2.4
T4	2.36	65	2
T4	2.36	65	1.6
T4	0.5	60	4.1
T5	2.36	50	DNF

Note: Grey values are confirmation data.

Appendix B. 1a.2 Raw Data

This appendix appears in its original form, without editorial change.

Strength	NaCl Conc.	Test Load	TTF
T1	0.5	85	DNF
T1	0.5	90	DNF
T1	0.5	85	DNF
T1	0.5	95	0.8
T1	0.5	95	0.01
T2	0.01	85	DNF
T2	0.01	85	DNF
T2	2.36	85	DNF
T2	2.36	95	0.03
T2	0.01	90	DNF
T2	0.01	95	43.4
T2	2.36	85	DNF
T2	2.36	90	DNF
T2	2.36	95	117.5
T2	0.01	95	DNF
T3	0	85	DNF
T3	0.5	85	6.4
T3	0	85	DNF
T3	0.5	95	0.7
T3	0.5	85	DNF
T3	0.5	95	0.01
T3	3.5	85	DNF
T3	0.5	95	0.2
T3	3.5	85	7
T3	0.5	85	DNF
T3	0.5	85	2.7
T3	0.5	75	DNF
T3	0.5	85	DNF
T3	0.5	75	8.9
T3	0	85	DNF
T3	0.5	75	DNF
T3	0.5	95	0.01
T3	0.5	85	4.9
T3	0.5	75	DNF
T3	0.5	85	DNF
T3	0.5	85	44.2
T3	3.5	85	6.3
T3	0	85	DNF
T3	0.5	85	35.8
T3	0.5	95	0.1
T3	0	85	DNF
T3	3.5	85	DNF
T3	0.5	75	DNF
T3	0.5	85	DNF
T3	0.5	85	DNF
T3	3.5	85	4.6
T3	0.5	85	3.4
T4	0.01	90	0.3
T4	2.36	60	DNF
T4	0.01	60	DNF
T4	2.36	90	0.07
T4	0.01	90	0.5
T4	0.01	60	DNF
T4	2.36	60	0.2
T4	2.36	75	0.2
T4	2.36	90	0.1
T4	0.01	75	114.7
T5	0.5	50	71.1
T5	0.5	80	0.2
T5	0.5	65	8.2
T5	0.5	50	166.2
T5	0.5	80	0.2
T1	3.5	90	DNF
T2	0	90	DNF
T2	0.5	85	DNF
T2	2.36	90	DNF
T2	3.5	85	DNF
T2	3.5	95	DNF
T3	3.5	80	DNF
T3	0	90	DNF
T3	0.5	80	82.1
T3	2.36	80	1.4
T4	0	75	19.9
T4	0.01	70	17.9
T4	0.5	70	18.1
T4	2.36	65	4.0
T4	3.5	60	0.2
T5	3.5	45	DNF

Note: Grey values are confirmation data.

Appendix C. 1c Raw Data

This appendix appears in its original form, without editorial change.

Strength	NaCl Conc.	Test Load	TTF
T1	0.5	85	DNF
T1	0.5	90	DNF
T1	0.5	85	DNF
T1	0.5	95	DNF
T1	0.5	95	DNF
T2	0.01	85	DNF
T2	0.01	85	DNF
T2	2.36	85	DNF
T2	2.36	95	DNF
T2	0.01	90	DNF
T2	0.01	95	DNF
T2	2.36	85	DNF
T2	2.36	90	DNF
T2	2.36	95	DNF
T2	0.01	95	DNF
T3	0	85	DNF
T3	0.5	85	DNF
T3	0	85	DNF
T3	0.5	95	DNF
T3	0.5	85	DNF
T3	0.5	95	DNF
T3	3.5	85	DNF
T3	0.5	95	0.1
T3	3.5	85	DNF
T3	0.5	85	DNF
T3	0.5	85	DNF
T3	0.5	75	DNF
T3	0.5	85	0.28
T3	0.5	75	DNF
T3	0	85	DNF
T3	0.5	75	DNF
T3	0.5	95	DNF
T3	0.5	85	DNF
T3	0.5	75	DNF
T3	0.5	85	DNF
T3	0.5	85	DNF
T3	3.5	85	0.77
T3	0	85	DNF
T3	0.5	85	DNF
T3	0.5	95	DNF
T3	0	85	DNF
T3	3.5	85	DNF
T3	0.5	75	DNF
T3	0.5	85	DNF
T3	0.5	85	DNF
T3	3.5	85	DNF
T4	0.01	90	0.5
T4	2.36	60	DNF
T4	0.01	60	DNF
T4	2.36	90	0.28
T4	0.01	90	6.0
T4	0.01	60	DNF
T4	2.36	60	DNF
T4	2.36	75	DNF
T4	2.36	90	1.7
T4	0.01	75	DNF
T5	0.5	50	DNF
T5	0.5	80	0.02
T5	0.5	65	24.6
T5	0.5	50	DNF
T5	0.5	80	0.04
T1	3.5	95	DNF
T2	0	95	DNF
T2	0.5	95	DNF
T2	3.5	95	DNF
T2	3.5	95	DNF
T2	3.5	95	DNF
T3	0	90	DNF
T3	0.5	95	DNF
T3	2.36	95	0.4
T3	3.5	95	175.6
T4	0	90	DNF
T4	0.01	85	3.6
T4	0.5	85	65.7
T4	2.36	85	DNF
T4	3.5	80	DNF
T5	3.5	50	DNF

Note: Grey values are confirmation data.

Appendix D. 1d Raw Data

This appendix appears in its original form, without editorial change.

Strength	NaCl Conc.	Test Load	TTF
T1	0.5	85	DNF
T1	0.5	90	DNF
T1	0.5	85	DNF
T1	0.5	95	DNF
T1	0.5	95	DNF
T2	0.01	85	DNF
T2	0.01	85	DNF
T2	2.36	85	DNF
T2	2.36	95	DNF
T2	0.01	90	DNF
T2	0.01	95	DNF
T2	2.36	85	DNF
T2	2.36	90	1.8
T2	2.36	95	58.6
T2	0.01	95	DNF
T3	0	85	DNF
T3	0.5	85	DNF
T3	0	85	DNF
T3	0.5	95	101
T3	0.5	85	165.6
T3	0.5	95	0.2
T3	3.5	85	0.4
T3	0.5	95	2.9
T3	3.5	85	1.3
T3	0.5	85	108.1
T3	0.5	85	DNF
T3	0.5	75	DNF
T3	0.5	85	120.7
T3	0.5	75	DNF
T3	0	85	DNF
T3	0.5	75	DNF
T3	0.5	95	95.6
T3	0.5	85	DNF
T3	0.5	75	DNF
T3	0.5	85	1.5
T3	0.5	85	DNF
T3	3.5	85	DNF
T3	0	85	59.3
T3	0.5	85	114.8
T3	0.5	95	7.9
T3	0	85	DNF
T3	3.5	85	DNF
T3	0.5	75	DNF
T3	0.5	85	DNF
T3	0.5	85	DNF
T3	3.5	85	0.3
T3	0.5	85	DNF
T4	0.01	90	0.1
T4	2.36	60	37.3
T4	0.01	60	48.9
T4	2.36	90	1.46
T4	0.01	90	0.01
T4	0.01	60	61.1
T4	2.36	60	72.2
T4	2.36	75	4.5
T4	2.36	90	0.2
T4	0.01	75	28.6
T5	0.5	50	21.4
T5	0.5	80	33.1
T5	0.5	65	15.0
T5	0.5	50	DNF
T5	0.5	80	24.9
T1	3.5	95	DNF
T2	0	90	DNF
T2	0.5	85	DNF
T2	2.36	90	DNF
T2	3.5	85	DNF
T2	3.5	95	BAD
T3	0	90	DNF
T3	0.5	80	DNF
T3	2.36	75	DNF
T3	3.5	75	DNF
T4	0	60	25.3
T4	0.01	55	163.2
T4	0.5	55	85.4
T4	2.36	55	46.4
T4	3.5	50	82.3
T5	3.5	45	DNF

Note: Grey values are confirmation data

Appendix E. 1e Raw Data

This appendix appears in its original form, without editorial change.

Strength	NaCl Conc.	Test Load	TTF
T1	0.5	85	DNF
T1	0.5	90	DNF
T1	0.5	85	DNF
T1	0.5	95	DNF
T1	0.5	95	DNF
T2	0.01	85	DNF
T2	0.01	85	DNF
T2	2.36	85	DNF
T2	2.36	95	DNF
T2	0.01	90	DNF
T2	0.01	95	DNF
T2	2.36	85	DNF
T2	2.36	90	DNF
T2	2.36	95	DNF
T2	0.01	95	DNF
T3	0	85	DNF
T3	0.5	85	DNF
T3	0	85	DNF
T3	0.5	95	DNF
T3	0.5	85	DNF
T3	0.5	95	0.9
T3	3.5	85	DNF
T3	0.5	95	3.1
T3	3.5	85	0.4
T3	0.5	85	DNF
T3	0.5	85	DNF
T3	0.5	75	DNF
T3	0.5	85	DNF
T3	0.5	75	DNF
T3	0	85	DNF
T3	0.5	75	DNF
T3	0.5	95	DNF
T3	0.5	85	DNF
T3	0.5	75	DNF
T3	0.5	85	DNF
T3	0.5	85	DNF
T3	3.5	85	DNF
T3	0	85	DNF
T3	0.5	85	9.3
T3	0.5	95	DNF
T3	0	85	DNF
T3	3.5	85	DNF
T3	0.5	75	DNF
T3	0.5	85	DNF
T3	0.5	85	DNF
T3	3.5	85	1.4
T3	0.5	85	DNF
T4	0.01	90	0.3
T4	2.36	60	71.1
T4	0.01	60	DNF
T4	2.36	90	0.2
T4	0.01	90	1.3
T4	0.01	60	5.4
T4	2.36	60	DNF
T4	2.36	75	70.6
T4	2.36	90	0.11
T4	0.01	75	23.4
T5	0.5	50	DNF
T5	0.5	80	5.6
T5	0.5	65	149.8
T5	0.5	50	DNF
T5	0.5	80	2.2
T1	3.5	95	DNF
T2	0	95	DNF
T2	0.5	95	DNF
T2	3.5	95	DNF
T2	3.5	95	DNF
T2	3.5	95	DNF
T3	3.5	90	DNF
T3	0	90	DNF
T3	0.5	95	DNF
T3	2.36	90	DNF
T4	0	75	DNF
T4	0.01	75	11.5
T4	0.5	75	1.6
T4	2.36	70	111.9
T4	3.5	60	DNF
T5	3.5	50	DNF

Note: Grey values are confirmation data.

NO. OF
COPIES ORGANIZATION

1 DEFENSE TECHNICAL
 (PDF INFORMATION CTR
 only) DTIC OCA
 8725 JOHN J KINGMAN RD
 STE 0944
 FORT BELVOIR VA 22060-6218

1 DIRECTOR
 US ARMY RESEARCH LAB
 IMNE ALC HRR
 2800 POWDER MILL RD
 ADELPHI MD 20783-1197

1 DIRECTOR
 US ARMY RESEARCH LAB
 RDRL CIO LL
 2800 POWDER MILL RD
 ADELPHI MD 20783-1197

1 DIRECTOR
 US ARMY RESEARCH LAB
 RDRL CIO LT
 2800 POWDER MILL RD
 ADELPHI MD 20783-1197

NO. OF
COPIES ORGANIZATION

6 US ARMY RDECOM
AVN ENGRNG DIRCTRT
MTRLS BR
STRUCTURES AND MATERIALS DIV
RDMR AEF
M KANE
D GRONER
G LIU
S WEBB
K HAMLIN
BLDG 4488 RM 211
REDSTONE ARSENAL AL 35898

2 US ARMY AMCOM
AMSAM ENV TI
M FEATHERS
L HASENBEIN
BLDG 111 RM 128
REDSTONE ARSENAL AL 35898

ABERDEEN PROVING GROUND

1 COMMANDER
ABERDEEN TEST CENTER
TEDT AT WFA
B HARDISKY
BLDG 400
APG MD 21005-5059

6 DIR USARL
RDRL WMM F
H MAUPIN
S GREND AHL
F KELLOGG
M MOTYKA
H NGUYEN
S FUDGER
BLDG 4600
APG MD 21005-5069